第41卷 第1期 岩 石 矿 物 学 杂 志 Vol. 41, No. 1: 1~17
2022年1月 ACTA PETROLOGICA ET MINERALOGICA Jan., 2022

·专题研究·

四川华蓥偏岩子晚二叠世玄武岩地球化学特征及其与峨眉山大火成岩省的成因关系

刘 冉[1,2],李 亚[2],赵立可[2],王 尉[2],李宏博[3,4],李常权[3],李博通[3]

(1. 中国石油大学(北京) 地球科学学院, 北京 102249; 2. 中国石油西南油气田分公司 勘探开发研究院, 四川 成都 610041; 3. 中国地质大学(北京) 中国地质大学地质过程与矿产资源国家重点实验室, 北京 100083; 4. 中国地质博物馆, 北京 100034)

摘 要: 四川华蓥偏岩子地区位于四川盆地中东部,新发现的晚二叠世玄武岩介于茅口组(下伏)和龙潭组(上覆)之间,可与峨眉山玄武岩进行对比。矿物学和地球化学研究表明,偏岩子玄武岩属于高钛亲碱性系列,具有OIB型的稀土元素和微量元素配分模式。偏岩子玄武岩基本未遭受地壳混染,单斜辉石的结晶温度为1 405~1 439℃,指示源区存在异常高温。稀土元素模拟结果表明,偏岩子玄武岩是峨眉山地幔柱在石榴子石-尖晶石过渡区经较低程度部分熔融的产物。总体上,偏岩子晚二叠世玄武岩与峨眉山玄武岩,尤其是峨眉山大火成岩省(ELIP)东部的玄武岩十分相似,是ELIP的组成部分。

关键词: 地球化学; 峨眉山大火成岩省; 玄武岩; 地幔柱; 四川偏岩子

中图分类号: P588.14+5; P59 **文献标识码**: A **文章编号**: 1000-6524(2022)01-0001-17

Geochemical characteristics of the Late Permian basalts in Pianyanzi, Huaying, Sichuan and their genetic relationship with Emeishan Large Igneous Province

LIU Ran[1,2], LI Ya[2], ZHAO Li-ke[2], WANG Wei[2], LI Hong-bo[3,4], LI Chang-quan[3] and LI Bo-tong[3]

(1. College of Geosciences, China University of Petroleum, Beijing 102249, China; 2. Exploration and Development Research Institute, PetroChina Southwest Oil & Gasfield Company, Chengdu 610041, China; 3. State Key Laboratory of Geological Processes and Mineral Resources, China University of Geosciences, Beijing 100083, China; 4. Geological Museum of China, Beijing 100034, China)

Abstract: Huaying Pianyanzi area is located in the middle-east of Sichuan Basin. The newly discovered Pianyanzi Late Permian basalt is between Maokou Formation (underlying) and Longtan Formation (overlying), which can be compared with Emeishan basalt. The study of petrology, mineralogy and geochemistry suggests that Pianyanzi basalts belong to the high-Ti alkaline series, and the rare earth element (REE) and trace element patterns are similar to those typically found in ocean island basalts (OIB). The basalts have not undergone any significant crustal contamination. The crystallization temperature of clinopyroxene is estimated to be 1 405~1 439℃, suggesting anomalously thermal inputs from a mantle source and a possible plume-head origin. The REE simulation result suggests that Pianyanzi basalts were produced by small degree of partial melting of Emeishan mantle plume within the garnet-spinel transition region. In general, the Pianyanzi Late Permian basalt is very similar to the Emeishan basalt, especially the basalt in the east of Emeishan Large Igneous Province (ELIP), which is an integral part of ELIP.

收稿日期: 2021-06-11; **接受日期**: 2021-10-19; **编辑**: 郝艳丽

基金项目: "十三五"国家重大专项(2016ZX05007004); 中国石油西南油气田公司科技重大专项(2019ZD01)

作者简介: 刘 冉(1990-), 男, 硕士研究生, 主要从事四川盆地油气勘探研究工作, E-mail: liuran01@petrochina.com.cn。

网络首发时间: 2021-11-22; **网络首发地址**: https://kns.cnki.net/kcms/detail/11.1966.P.20211119.1904.002.html

Key words: geochemistry; Emeishan Large Igneous Province; basalt; mantle plume; Pianyanzi, Sichuan
Fund support: Major National Special Project in the 13th Five-Year Plan (2016ZX05007004); Major Science and Technology Project of PetroChina Southwest Oil & Gasfield Company (2019ZD01)

大火成岩省(LIPs)是地球演化历史中的重大地质事件,以短时间内的巨量喷发为特征(Bryan and Ernst, 2008),一般认为LIPs的形成与地幔柱作用有关(Hill, 1991; Farnetani and Richards, 1994; Farnetani, 1996; Cordery *et al.*, 1997; Courtillot *et al.*, 1999; Olsen, 1999)。在LIPs的研究中,岩浆作用的规模(分布面积或延伸范围)是一个十分重要的参数,也是评判一个溢流玄武岩区能否被定义为大火成岩省的重要指标(Ernst *et al.*, 2005; Sheth, 2007; Bryan and Ernst, 2008)。此外,大火成岩省的规模对于大火成岩省体积的估算、大火成岩省的起源(地幔柱/非地幔柱模型等)、地幔柱头部规模的限定以及大火成岩省所产生的环境影响等科学问题,都具有十分重要的意义(Griffiths *et al.*, 1989; Campbell and Griffiths, 1990; Hill, 1991; Griffiths and Campbell, 1991; Coffin and Eldholm, 1994, 2001; Kincaid *et al.*, 1996; Campbell, 1998, 2001; Davies, 2000; Ernst and Buchan, 2001a, 2001b, 2002, 2003; Courtillot *et al.*, 2003; Hames *et al.*, 2003; Sheth, 2007; Bryan and Ernst, 2008; Zhu *et al.*, 2021a, 2021b)。

位于中国西南的二叠纪峨眉山大火成岩省(ELIP)一般被认为是一次地幔柱事件的产物(Chung and Jahn, 1995; He *et al.*, 2003; Song *et al.*, 2004; Xiao *et al.*, 2004a; Xu *et al.*, 2004, 2008; Zhang *et al.*, 2006, 2008; Shellnutt *et al.*, 2008)。相比于其他面积均超过1×10^6 km^{2}的典型LIPs(例如Ontong Java、Siberain、Karoo-Ferrar、Deccan, Coffin and Eldholm, 1994; Ernst, 2014),ELIP的出露面积相对较小,仅为2.5×10^5 km^2(张云湘等, 1988; Xu *et al.*, 2001),这也引起了对ELIP地幔柱模型的质疑(Ali *et al.*, 2004)。由于漫长地质历史中的构造破坏和风化剥蚀作用,现今所见到的仅是ELIP的一部分,而ELIP的实际面积很可能要大得多。近年来,ELIP周边地区的晚二叠世玄武岩被相继发现,并被认为是ELIP的组成部分(图1),例如,ELIP北-西北部宝兴地区的大石包组玄武岩(Xiao *et al.*, 2004b; Zi *et al.*, 2010)、ELIP西部香格里拉地区的冈达概组玄武岩(吕劲松等, 2013)、ELIP南-东南方向越南北部Song Da地区和广西田林-巴马地区的玄武岩(Polyakov *et al.*, 1998; Hanski *et al.*, 2004, 2010; Fan *et al.*, 2008)。这些玄武岩的发现扩大了人们对ELIP分布范围原有的认识。

ELIP的东北部,即四川盆地地区,由于中生代—新生代沉积地层的覆盖,鲜有二叠纪地层出露(刘德良等, 2000)。但据区域地质调查以及油气钻探资料显示,在川东的威远、珙县、广安(华蓥山)以及重庆南川等地有晚二叠世玄武岩(或凝灰岩)出露(童崇光, 1992; 四川省地质矿产局, 1995❶; Ma *et al.*, 2008; 张招崇, 2009; 田和明等, 2014; 陈辉等, 2019; Wen *et al.*, 2019; Xiang *et al.*, 2021)。然而,对这些玄武岩还缺乏系统的研究工作,它们与峨眉山大火成岩省之间的成因关系也不明确。近期,笔者在四川华蓥偏岩子又发现了晚二叠世玄武岩出露,对其进行了矿物学、地球化学特征的研究,欲揭示其与峨眉山玄武岩之间的成因关系,从而为ELIP分布范围界定以及探究峨眉山地幔柱地球动力学特征提供重要信息。

1 地质背景

1.1 峨眉山大火成岩省

峨眉山大火成岩省(ELIP)位于中国西南地区,西藏高原的东部,扬子克拉通的西缘(图1)。ELIP呈菱形分布,由广布的大陆溢流拉斑玄武质熔岩(包括少量苦橄岩、安山质玄武岩)以及同期侵位的超基性-基性(放射状岩墙群)以及中酸性岩体组成(Chung *et al.*, 1998; Zhou *et al.*, 2002, 2005; Zhong *et al.*, 2004; 李宏博等, 2010, 2015; Li *et al.*, 2015),熔岩的厚度呈西厚(>5 km)东薄(仅几百米)的变化趋势(Chung and Jahn, 1995; Xu *et al.*, 2001; Xiao *et al.*, 2004a; Zhang *et al.*, 2006)。传统观点认为,ELIP的西北和西南边界为龙门山和哀牢山-红河断裂带,而东界在贵阳以东的福泉至瓮安一线,东北界和东南界分别受宝兴-宜宾断裂和弥

❶ 四川省地质矿产局. 1995. 中和镇幅 H-48-70-A 1:5万地质图说明书.

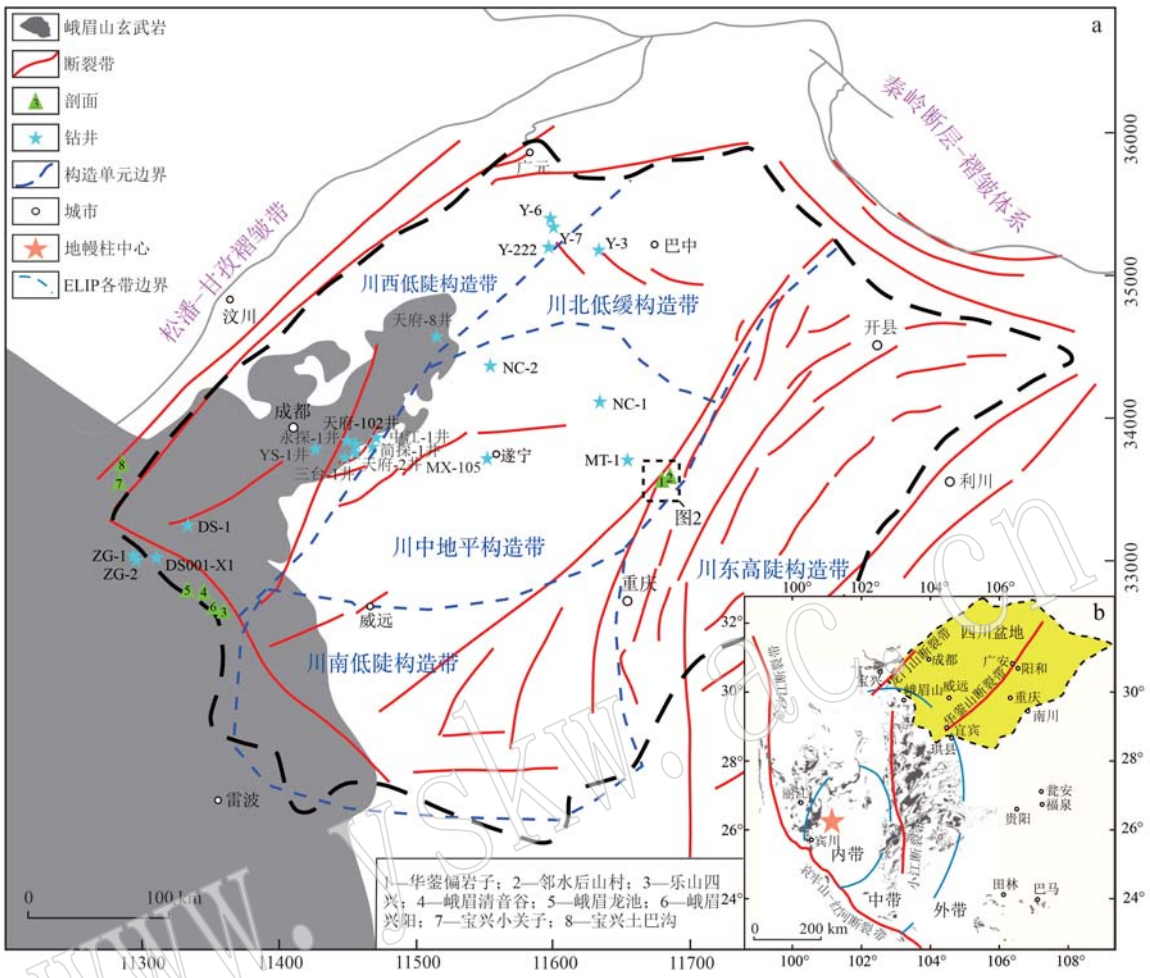

图 1　四川盆地构造简图、晚二叠世玄武岩出露点/钻井分布图[a,底图据殷积峰等(2013)、Ma 等(2019)，玄武岩出露点和钻井据 Li 等(2016，2017)、陈辉等(2019)、Wen 等(2019)、刘冉等(2021)和 Xiang 等(2021)]和峨眉山大火成岩省与四川盆地地理位置图[b,底图据 Li 等(2017)]

Fig. 1　Structural map of Sichuan Basin and distribution of outcrops/wells of Late Permian basalts (a, base map after Yin Jifeng *et al.*, 2013; Ma *et al.*, 2019; outcrops/wells after Li *et al.*, 2016, 2017; Chen *et al.*, 2019; Wen *et al.*, 2019; Liu Ran *et al.*, 2021; Xiang *et al.*, 2021) and location map of Emeishan Large Igneous Province and Sichuan Basin (b, after Li *et al.*, 2017)

勒-斯宗断裂所控制(图 1；Chung *et al.*，1998；Xu *et al.*，2001；宋谢炎等，2002；肖龙等，2003)。

峨眉山玄武岩与下伏的中二叠统茅口组灰岩呈喷发不整合接触，与上覆的上二叠统宣威组或龙潭组呈整合/不整合接触关系(肖龙等，2003；李宏博等，2011)。根据峨眉山玄武岩下伏的茅口组灰岩差异剥蚀的情况，He 等(2003)将 ELIP 由内至外划分为内带、中带和外带(图 1)，这与 ELIP 地壳厚度的估计以及地震波速带的分布情况是吻合的(Xu *et al.*，2004；Chen *et al.*，2015)。从近年来对 ELIP 的同位素年代学研究获得的一些高精度年龄结果来看，峨眉山玄武岩的主喷发期在 260～257 Ma 之间，其中喷发峰期在 260 Ma 左右 (Zhou *et al.*，2006，2008；He *et al.*，2007；Fan *et al.*，2008；Xu *et al.*，2008；朱江等，2011；李宏博等，2012；Shellnutt *et al.*，2012；Zhong *et al.*，2014；Li *et al.*，2015)，但也有学者认为结束于二叠纪末期 (朱江等，2011)。

1.2　偏岩子地区地质概况

四川华蓥偏岩子地区位于扬子克拉通以及四川盆地的腹地(图 1)。基底可能是中上元古界沉积变质岩系，喜山运动使得该区寒武系至第四系(除了白垩系)的沉积盖层全部褶皱隆升并出露，其中上二叠统出露的地层主要包括中二叠统茅口组(P_2m)灰岩、上二叠统峨眉山玄武岩($P_3\beta$)以及龙潭组(P_3l)(图 2、图 3a)。NE-SW 向的华蓥山深大断裂带不仅是四川盆地内唯一的一条贯穿岩石圈的深大断裂

带,也是区内晚二叠世峨眉山玄武岩的主要控制构造单元和喷发通道(四川省地质矿产局, 1995❶; 李洪奎, 2020)。

晚二叠世玄武岩是区内唯一的岩浆活动的产物,在华蓥山一带呈断续分布,一般厚 10~50 m,位于龙潭组之下,茅口组之上,与两者均为平行不整合接触(图 2; 四川省地质矿产局, 1995)❶,与区域上峨眉山玄武岩的产出位置相同。区内出露的茅口组为灰白色厚层、块状微晶灰岩及灰色中至厚层状含燧石团块灰岩,产蜓 *Neoschwageiina Craticulifera*,但缺失 *Yabeina-Neomisellina* 顶峰亚带的标准化石 *Yabeina* 和 *Neomisellina*,说明茅口组灰岩遭受了强烈的剥蚀作用(四川省地质矿产局, 1995)❶,这与云南宾川、弥渡蔡家地 ELIP 内带峨眉山玄武岩剖面的情况一致(覃建雄等, 1999; He *et al.*, 2003)。

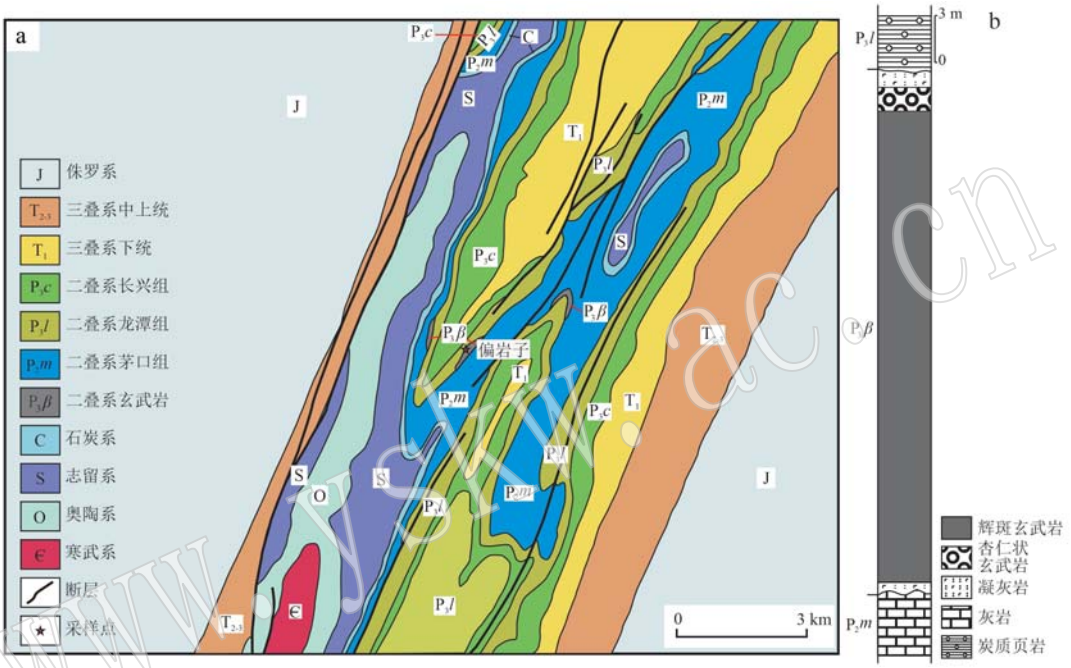

图 2 四川偏岩子地区晚二叠世玄武岩地质图(a, 据四川省地质矿产局, 1995)❶和剖面柱状图(b)

Fig. 2 Geological map of Late Permian Pianyanzi basalts in Sichuan Province (a, after SBGMR, 1995) ❶ and Section and column map(b)

1.3 偏岩子玄武岩产状及岩相特征

新发现的偏岩子晚二叠世玄武岩层出露厚度约 30 m,产状 98°∠32°,顶部发育杏仁状玄武岩(图 2、图 3)。上覆地层为龙潭组炭质页岩、粉砂质页岩、硅质灰岩,下伏地层为茅口组灰岩。玄武岩与上下地层均为喷发不整合接触。玄武岩呈铁灰色,柱状节理发育,岩石十分新鲜,基本未见蚀变(图 3a~3c)。偏岩子玄武岩的斑晶主要为斜长石和单斜辉石,另有少量的 Fe-Ti 氧化物(磁铁矿和钛铁矿,含量 5%~10%)。斜长石斑晶为自形晶,粒径一般为 1.5~2 mm,含量 40%~50%; 辉石斑晶为半自形至它形,偶见自形晶体,粒径一般 1.5~2.0 mm,个别达 3 mm,含量 20%~30%。玄武岩的基质结晶程度良好,表现为全晶质结构(图 3d、3e)。

2 测试方法

本次研究采集的样品来自四川偏岩子剖面(图 2、图 3)。矿物的电子探针成分测试在中国地质大学(北京)电子探针室完成,仪器型号为日本岛津 EPMA-1600 型电子探针仪,测试电压为 15 kV,电流为 1×10^{-7} mA,束斑直径为 1 μm,主量元素测试相对误差≤5%,标准样品为 Si、Al、Na(钠长石)、Ti(金红石)、Fe(铁铝榴石)、Mn(蔷薇辉石)、Ca(方解石)、K(透长石)、Rb(铯榴石),均为美国 SPI 公司研制的电子探针标准物质。

❶ 四川省地质矿产局. 1995. 中和镇幅 H-48-70-A 1:5 万地质图说明书.

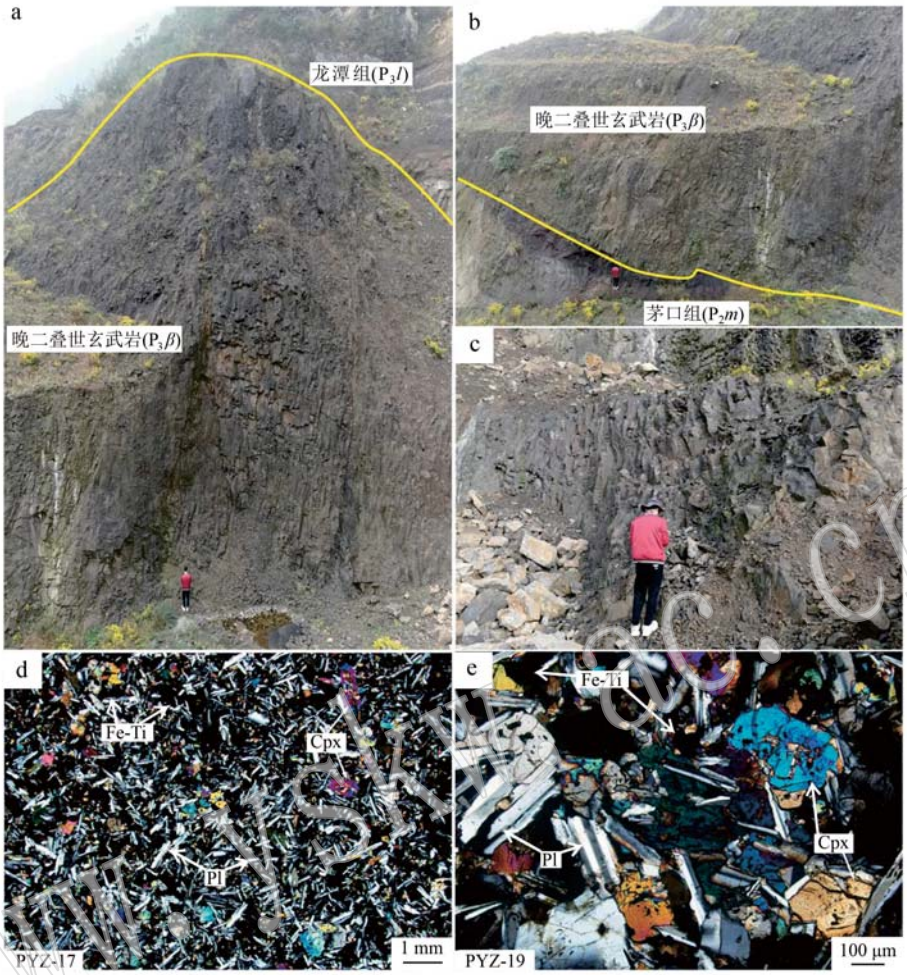

图 3　四川华蓥晚二叠世玄武岩野外和镜下照片

Fig. 3　Representative field photos and photomicrographs of the Late Permian basalts in the Pianyanzi, Huaying, Sichuan

a—偏岩子剖面,晚二叠世玄武岩与上覆的晚二叠世龙潭组(P_3l)呈平行不整合接触; b—晚二叠世玄武岩与下覆的中二叠世茅口组(P_2m)呈平行不整合接触; c—玄武岩的柱状节理; d—具典型间粒结构的玄武岩(正交偏光); e—自形-半自形的单斜辉石(Cpx)斑晶,长板状的斜长石(Pl)斑晶以及铁钛氧化物(Fe-Ti)(正交偏光)

a—the Upper Permian Longtan Formation (P_3l) unconformably lying over the Late Permian basalt, Pianyanzi section; b—eruptive unconformity between the Late Permian basalt and the Middle Permian Maokou Formation (P_2m); c—columnar joint of basalt; d—basalt with intergranular texture (cross-polarized light); e—euhedral-subhedral clinopyroxene(Cpx) phenocryst distributing in lath-shaped plagioclase(Pl) and anhedral fine-grained Fe-Ti oxides(Fe-Ti) (cross-polarized light)

全岩分析在武汉上谱分析科技有限责任公司进行,主量元素分析仪器使用日本理学(Rigaku)生产的 ZSX Primus Ⅱ型波长色散 X 射线荧光光谱仪(XRF),4.0 kW 端窗铑靶 X 射线光管,电压 50 kV,电流 60 mA,分析谱线均为 Kα,标准曲线使用国家标准物质岩石系列 GBW07101-14、土壤系列 GBW07401-08、水系沉积物系列 GBW07302-12 建立,数据校正采用理论 α 系数法,测试相对标准偏差(RSD)<2%。

3　分析结果

3.1　矿物学特征

偏岩子玄武岩中代表性的单斜辉石、斜长石以及 Fe-Ti 氧化物的电子探针成分分析结果分别列于表 1、表 2 和表 3 中。

电子探针成分分析结果显示,偏岩子玄武岩辉石($Wo_{38\sim43}En_{36\sim42}Fs_{17\sim23}$)成分变化不大,其中 TiO_2

表 1 四川华蓥偏岩子玄武岩单斜辉石电子探针分析结果 w_B/%

Table 1 EPMA analysis results of clinopyroxene in Pianyanzi basalts

样品号	PYZ16		PYZ18		PYZ20		PYZ21		PYZ23		PYZ25		PYZ26	
点号	PYZ16-1	PYZ16-2	PYZ18-1	PYZ18-2	PYZ20-1	PYZ20-2	PYZ21-1	PYZ21-2	PYZ23-1	PYZ23-2	PYZ25-1	PYZ25-2	PYZ26-1	PYZ26-2
SiO_2	49.46	48.75	47.42	48.73	48.37	48.65	47.45	46.91	47.71	48.44	48.05	49.39	46.72	50.14
TiO_2	1.16	1.60	1.71	1.26	1.26	1.15	1.71	1.44	1.22	1.13	1.22	1.21	2.21	0.97
Al_2O_3	2.45	3.56	3.17	2.74	2.66	2.63	4.12	4.91	2.54	2.70	2.63	2.21	4.68	2.39
Cr_2O_3	0.08	0.16	0.05	0.09	0.22	0.15	0.13	0.20	0.46	0.11	1.97	0.04	0.00	0.05
FeO	10.65	11.38	11.50	11.44	11.04	11.01	10.87	11.43	14.09	11.09	11.19	11.40	12.60	11.65
MnO	0.24	0.29	0.28	0.24	0.25	0.25	0.25	0.32	0.29	0.26	0.24	0.33	0.35	0.26
MgO	14.50	13.91	13.42	13.88	14.19	13.75	13.87	13.74	12.67	13.79	13.77	13.95	12.48	15.17
CaO	21.18	20.65	20.71	21.48	20.82	21.06	20.13	19.55	19.83	20.86	20.99	20.96	20.63	19.25
Na_2O	0.35	0.35	0.38	0.36	0.39	0.32	0.43	0.42	0.34	0.38	0.36	0.88	0.41	0.37
K_2O	0.01	0.01	0.00	0.02	0.01	0.01	0.02	0.00	0.04	0.02	0.00	0.20	0.00	0.00
总计	100.08	100.66	98.64	100.24	99.21	98.98	98.98	98.92	99.19	98.78	100.42	100.57	100.08	100.25
以6个氧原子和4个阳离子为基准														
Si	1.868 2	1.835 4	1.829 5	1.848 9	1.849 8	1.863 3	1.814 9	1.797 7	1.849 2	1.860 1	1.826 5	1.868 4	1.785 7	1.885 4
$Al^{(Ⅳ)}$	0.032 9	0.045 3	0.049 7	0.035 9	0.036 3	0.033 0	0.185 2	0.202 3	0.035 6	0.032 7	0.034 9	0.034 4	0.063 6	0.027 4
$Al^{(Ⅵ)}$	–	–	–	–	–	–	0.000 5	0.019 4	–	–	–	–	–	–
Ti	0.032 9	0.045 3	0.049 7	0.035 9	0.036 3	0.033 0	0.049 2	0.041 6	0.035 6	0.032 7	0.034 9	0.034 4	0.063 6	0.027 4
Cr	0.002 5	0.004 8	0.001 5	0.002 6	0.006 7	0.004 4	0.003 9	0.006 0	0.013 9	0.003 2	0.059 3	0.001 3	0	0.001 4
Fe^{3+}	0.165 9	0.150 7	0.184 1	0.195 5	0.193 2	0.160 4	0.169 4	0.184 4	0.189 1	0.175 7	0.186 4	0.247 9	0.178 8	0.139 7
Fe^{2+}	0.166 0	0.203 0	0.181 2	0.161 7	0.154 3	0.187 7	0.173 4	0.176 3	0.260 6	0.175 2	0.163 7	0.105 2	0.218 0	0.222 2
Mn	0.007 6	0.009 1	0.009 3	0.007 7	0.008 2	0.008 1	0.008 2	0.010 2	0.009 5	0.008 5	0.007 6	0.010 5	0.011 5	0.008 1
Mg	0.816 4	0.780 7	0.772 1	0.785 0	0.809 1	0.785 3	0.790 6	0.784 9	0.731 9	0.789 1	0.780 5	0.786 7	0.711 3	0.850 3
Ca	0.857 1	0.833 2	0.856 3	0.873 4	0.853 0	0.864 2	0.824 9	0.802 8	0.823 5	0.858 1	0.854 7	0.849 5	0.844 7	0.775 3
Na	0.025 6	0.025 8	0.028 7	0.026 3	0.029 2	0.024 0	0.031 5	0.031 1	0.025 6	0.028 6	0.026 2	0.064 6	0.030 2	0.026 9
K	0.000 3	0.000 3	0.000 1	0.001 0	0.000 3	0.000 3	0.000 7	–	0.002 0	0.001 1	–	0.009 8	–	0.000 2
总计	3.975 4	3.933 6	3.962 2	3.973 9	3.976 4	3.963 7	4.052 4	4.056 7	3.976 5	3.965 0	3.974 7	4.012 7	3.9074	3.964 3
Wo	42.05	41.61	42.15	42.61	41.67	42.58	41.29	40.35	40.36	42.17	42.33	41.15	42.35	38.33
En	40.05	38.99	38.00	38.30	39.53	38.69	39.57	39.45	35.87	38.77	38.66	38.11	35.66	42.04
Fs	16.65	18.12	18.44	17.80	17.38	17.55	17.56	18.64	22.51	17.66	17.71	17.61	20.47	18.30

–表示未计算出该数据。

表 2 四川华蓥偏岩子玄武岩斜长石电子探针分析结果 w_B/%

Table 2 EPMA analysis results of plagioclase in Pianyanzi basalts

样品号	PYZ16		PYZ18		PYZ20		PYZ21		PYZ23		PYZ25		PYZ26	
点号	PYZ16-1	PYZ16-2	PYZ18-1	PYZ18-2	PYZ20-1	PYZ20-2	PYZ21-1	PYZ21-2	PYZ23-1	PYZ23-2	PYZ25-1	PYZ25-2	PYZ26-1	PYZ26-2
SiO_2	56.57	52.40	53.60	51.06	52.40	50.32	50.82	52.64	52.32	51.81	50.75	53.61	51.59	52.61
TiO_2	0.20	0.11	0.17	0.22	0.08	0.17	0.10	0.08	0.06	0.08	0.12	0.13	0.10	0.12
Al_2O_3	25.51	28.80	28.06	29.91	28.57	28.55	30.50	29.30	28.52	29.38	29.39	27.70	30.05	28.26
FeO	1.02	1.01	0.84	0.85	0.90	0.86	0.80	0.96	0.81	1.36	0.74	0.95	0.85	0.68
MnO	0.01	0.05	0.05	0.00	0.03	0.05	0.01	0.01	0.04	0.02	0.06	0.00	0.01	0.00
MgO	0.09	0.11	0.12	0.11	0.14	0.12	0.12	0.12	0.13	0.28	0.10	0.13	0.12	0.14
CaO	8.13	11.86	11.04	13.13	11.83	12.43	13.45	12.16	11.79	12.54	12.72	10.49	13.21	11.94
Na_2O	6.57	4.71	5.29	4.25	4.75	4.30	4.13	4.85	4.83	4.56	4.31	5.41	4.22	4.73
K_2O	0.86	0.38	0.47	0.30	0.38	0.35	0.29	0.41	0.39	0.30	0.34	0.51	0.30	0.37
总计	98.96	99.43	99.64	99.84	99.06	97.15	100.21	100.53	98.88	100.33	98.53	98.91	100.44	98.86
以32个氧原子为基准														
Si	2.603 0	2.420 0	2.463 5	2.355 9	2.425 4	2.384 6	2.334 5	2.405 4	2.424 7	2.387 3	2.367 7	2.479 2	2.361 7	2.435 8
Al	1.383 2	1.567 5	1.519 9	1.626 5	1.558 7	1.594 3	1.651 3	1.578 0	1.557 6	1.595 8	1.615 8	1.509 7	1.621 6	1.542 0
Ca	0.401 0	0.586 7	0.543 7	0.649 3	0.586 8	0.631 3	0.661 9	0.595 2	0.585 6	0.619 0	0.635 8	0.519 6	0.648 2	0.592 2
Na	0.585 8	0.422 1	0.471 1	0.380 5	0.426 3	0.395 1	0.367 6	0.430 0	0.434 0	0.407 5	0.389 8	0.484 8	0.374 2	0.424 3
K	0.050 5	0.022 2	0.027 6	0.017 7	0.022 2	0.021 2	0.016 8	0.024 1	0.023 1	0.017 9	0.020 5	0.030 1	0.017 6	0.022 0
An	38.66	56.91	52.16	61.98	56.68	60.26	63.26	56.72	56.16	59.27	60.78	50.22	62.33	57.02
Ab	56.48	40.94	45.20	36.33	41.18	37.71	35.13	40.98	41.62	39.02	37.27	46.86	35.98	40.86
Or	4.87	2.15	2.64	1.69	2.14	2.03	1.61	2.29	2.21	1.71	1.96	2.91	1.70	2.12

表 3　四川华蓥偏岩子玄武岩 Fe-Ti 氧化物电子探针分析结果　　w_B/%

Table 3　EPMA analysis results of Fe-Ti oxides in Pianyanzi basalts

样品号	PYZ16		PYZ18		PYZ20		PYZ21		PYZ23		PYZ25		PYZ26	
点号	PYZ16-1	PYZ16-2	PYZ18-1	PYZ18-2	PYZ20-1	PYZ20-2	PYZ21-1	PYZ21-2	PYZ23-1	PYZ23-2	PYZ25-1	PYZ25-2	PYZ26-1	PYZ26-2
SiO_2	0.45	0.63	1.45	4.23	2.74	0.29	0.18	0.09	1.59	0.69	3.66	4.07	0.24	5.14
TiO_2	22.62	22.53	23.48	26.96	24.64	24.28	22.50	20.79	23.85	29.53	29.23	30.92	23.00	29.81
Al_2O_3	1.81	1.89	2.32	3.08	2.29	2.11	2.81	2.06	2.03	2.53	1.77	1.37	0.83	1.19
FeO	69.07	69.50	65.95	58.08	65.21	67.56	69.58	72.12	68.09	62.90	57.08	59.62	70.86	56.21
MnO	1.30	1.24	1.26	1.33	1.52	1.53	0.74	0.67	1.58	0.47	0.82	1.49	1.96	0.90
MgO	0.04	0.14	0.22	1.41	0.42	0.06	0.05	0.03	0.24	0.10	1.01	0.90	0.03	1.13
CaO	0.11	0.20	0.15	0.19	0.09	0.14	0.12	0.07	0.10	0.21	0.22	0.27	0.13	0.39
Na_2O	0.02	0.03	0.08	0.08	0.05	0.03	0.07	0.04	0.08	0.04	0.08	0.02	0.04	0.07
K_2O	0.02	0.03	0.01	0.03	0.04	0.04	0.04	0.00	0.03	0.02	0.04	0.03	0.00	0.05
Cr_2O_3	0.05	0.11	0.59	0.15	0.13	0.19	0.28	0.22	0.12	0.08	0.08	0.13	0.07	0.11
NiO	0.07	0.02	0.02	0.00	0.00	0.05	0.05	0.10	0.00	0.00	0.03	0.04	0.11	0.00
CoO	0.06	0.15	0.14	0.04	0.08	0.08	0.06	0.23	0.16	0.07	0.10	0.02	0.08	0.09
Total	95.62	96.48	95.66	95.58	97.20	96.37	96.48	96.44	97.88	96.63	94.13	98.86	97.34	95.08
Si	0.017	0.024	0.055	0.158	0.102	0.011	0.007	0.003	0.059	0.026	0.141	0.149	0.009	0.195
Ti	0.648	0.639	0.670	0.758	0.689	0.691	0.637	0.591	0.666	0.840	0.845	0.853	0.651	0.851
Al	0.081	0.084	0.104	0.135	0.100	0.094	0.125	0.092	0.089	0.113	0.080	0.059	0.037	0.053
Fe^{3+}	0.585	0.585	0.427	0.027	0.312	0.494	0.578	0.711	0.456	0.152	−0.056	−0.068	0.639	−0.152
Fe^{2+}	1.616	1.607	1.665	1.787	1.716	1.643	1.611	1.567	1.657	1.836	1.891	1.895	1.589	1.937
Mn	0.042	0.040	0.040	0.042	0.048	0.049	0.024	0.021	0.050	0.015	0.027	0.046	0.063	0.029
Mg	0.002	0.008	0.012	0.078	0.023	0.003	0.003	0.002	0.013	0.006	0.058	0.049	0.002	0.064
Ca	0.005	0.008	0.006	0.008	0.004	0.006	0.005	0.003	0.004	0.009	0.009	0.010	0.005	0.016
Na	0.001	0.002	0.006	0.005	0.004	0.002	0.005	0.003	0.006	0.003	0.006	0.001	0.003	0.005
K	0.001	0.001	0.001	0.002	0.002	0.002	0.002	0.000	0.002	0.001	0.002	0.001	0.000	0.002
Cr	0.002	0.003	0.018	0.004	0.004	0.006	0.008	0.007	0.004	0.002	0.002	0.004	0.002	0.003
Ba	0.000	0.000	0.000	0.000	0.000	0.000	0.000	0.000	0.000	0.000	0.000	0.000	0.000	0.000
Zn	0.000	0.000	0.000	0.000	0.000	0.000	0.000	0.000	0.000	0.000	0.000	0.000	0.000	0.000
V	0.000	0.000	0.000	0.000	0.000	0.000	0.000	0.000	0.000	0.000	0.000	0.000	0.000	0.000
Ni	0.002	0.001	0.001	0.000	0.000	0.002	0.001	0.003	0.000	0.000	0.001	0.001	0.003	0.000
Nb	0.000	0.000	0.000	0.000	0.000	0.000	0.000	0.000	0.000	0.000	0.000	0.000	0.000	0.000
Total	3.002	3.002	3.004	3.004	3.004	3.003	3.005	3.003	3.004	3.002	3.005	3.002	3.003	3.004

含量为 0.97%～2.21%，Al_2O_3 含量为 2.21%～4.91%，Na_2O 含量为 0.32%～0.88%（表 1），除 1 个点之外，均投在透辉石的范围之中（图 4）。在镜下未见辉石环带，这可能表明在熔岩喷发之前，辉石与熔体已经达到了平衡。根据 Putirka 等（2003）的单斜辉石温度计，估算了偏岩子玄武岩单斜辉石在岩浆房中的结晶温度，结果为 1 405～1 439℃。偏岩子玄武岩的斜长石成分有一定变化，主要是拉长石和中长石（$Ab_{39\sim63}An_{35\sim56}Or_{1.61\sim4.87}$）（表 2）。偏岩子玄武岩中 Fe-Ti 氧化物中 TiO_2 含量为 20.79%～30.92%，FeO^T 含量为 56.21%～72.12%，属于钛磁铁矿（表 3）。

3.2　主、微量元素特征

偏岩子玄武岩样品的全岩主、微量元素分析结果列于表 4。由表 4 可见，玄武岩样品的主量元素成分变化不大，其中 SiO_2 含量为 46.15%～48.88%，TiO_2 含量为 3.02%～3.25%，Al_2O_3 含量为 13.30%～13.68%，TFe_2O_3 含量为 14.71%～16.23%，MgO 含量为 4.07%～5.48%，CaO 含量为 9.38%～10.00%，全碱含量（Na_2O+K_2O）为 3.32%～4.38%，P_2O_5 含量为 0.39%～0.42%。按照峨眉山玄武岩高钛型和低钛型的划分标准（Xu *et al.*, 2001），偏岩子玄武岩属于高钛型。$Mg^{\#}$ 值为 35～42，表明经过了较大程度的演化。从 TAS 图解来看，偏岩子玄武岩基本都投在了亚碱性-玄武岩的范围之内，但是样品投点均十分靠近亚碱性-碱性的界限（图 5a）。因此，尽管镜下未发现有橄榄石斑晶，但偏岩子玄武岩在 Zr/TiO_2-Nb/Y 图中都投在了碱性玄武岩的范围之内（图 5b），说明偏岩子玄武岩具有较明显的亲碱性特征。总体来说，偏岩子玄武岩的主量元素特征与 ELIP 东部的玄武岩（贵州和广西的玄武岩，Fan *et al.*, 2008；Qi and Zhou, 2008；Lai *et al.*, 2012；廖宝丽等，2012）是相似的。

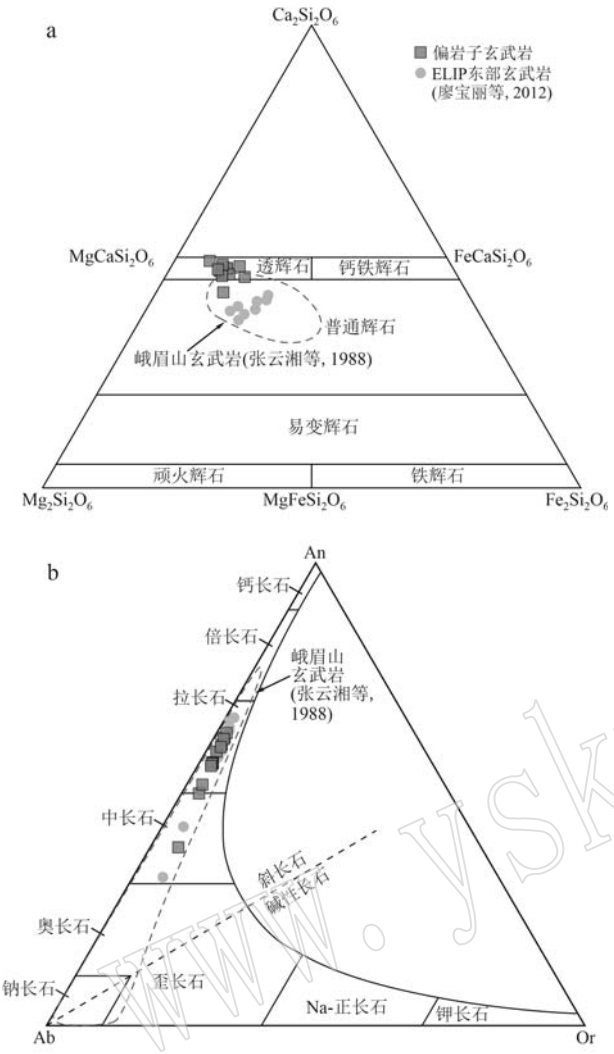

图4 偏岩子晚二叠世玄武岩中单斜辉石成分判别图解(a, Morimoto *et al.*, 1988)和An－Ab－Or长石成分判别图解(b, Smith and Brown, 1974)

Fig. 4 Wo－En－Fs diagram of clinopyroxene composition (a, Morimoto *et al.*, 1988) and An－Ab－Or diagram of feldspar composition (b, Smith and Brown, 1974) of Late Permian Pianyanzi basalts

4 讨论

4.1 岩浆演化和地壳混染

由于分离结晶(或堆晶)和地壳混染会对不相容元素的含量和比值造成影响,因此,在利用地球化学工具对偏岩子玄武岩的源区特征进行研究之前,首先要对分离结晶和地壳混染情况进行讨论。

偏岩子玄武岩具有较低的$Mg^{\#}$值(35~42),表明经历了较大程度的演化。结合镜下观察(图3d、3e),

表4 四川偏岩子晚二叠世玄武岩全岩主量(w_B/%)、微量元素含量($w_B/10^{-6}$)分析数据表

Table 4 Data of major (w_B/%) and trace elements ($w_B/10^{-6}$) of Late Permian Pianyanzi basalts

样品号	PYZ-16	PYZ-18	PYZ-20	PYZ-22	PYZ-24	PYZ-26
SiO_2	48.88	47.40	49.05	47.93	47.75	46.15
TiO_2	3.21	3.21	3.25	3.02	3.22	3.18
Al_2O_3	13.58	13.30	13.62	13.44	13.43	13.68
TFe_2O_3	15.10	16.25	14.71	15.88	14.88	15.72
MnO	0.22	0.24	0.21	0.23	0.24	0.23
MgO	4.13	4.82	4.07	4.86	5.48	4.44
CaO	9.56	9.60	9.49	9.81	9.99	9.38
Na_2O	3.12	2.85	3.11	2.69	2.69	3.11
K_2O	1.25	0.89	1.28	0.88	0.63	0.76
P_2O_5	0.41	0.41	0.42	0.39	0.39	0.41
LOI	0.52	0.78	0.47	0.99	1.26	2.37
Total	99.99	99.73	99.67	100.13	99.94	99.41
$Mg^{\#}$	35	37	35	38	42	36
Rb	27.6	10.3	27.9	10.2	5.9	18.1
Sr	466	504	453	478	410	401
Ba	370	396	387	411	318	315
Th	5.64	5.54	5.75	5.19	5.04	5.39
U	1.24	1.27	1.38	1.32	1.18	1.65
Nb	40.1	39.4	41.3	37.1	37.0	38.9
Ta	2.38	2.39	2.43	2.18	2.21	2.31
Zr	260	258	273	233	238	243
Hf	6.60	6.62	7.02	6.03	6.11	6.07
Y	39.7	38.7	39.7	38.0	36.7	35.0
Sc	29.2	29.0	29.5	30.1	29.8	30.1
Co	43.0	46.6	43.7	44.3	44.7	42.6
Ni	49.2	51.6	50.7	51.1	50.3	46.4
Cu	304	307	312	289	289	317
Pb	5.25	5.04	5.17	4.91	4.93	13.00
Zn	130	131	132	127	131	132
V	401	399	405	400	413	410
Cr	33.3	33.9	35.1	38.0	37.0	37.2
La	40.2	40.3	41.4	36.8	37.2	34.5
Ce	83.8	83.3	87.4	75.6	77.3	71.8
Pr	10.3	10.3	10.6	9.21	9.38	8.78
Nd	42.6	42.6	42.7	38.1	38.7	36.0
Sm	9.01	8.76	9.18	8.04	8.14	7.54
Eu	2.78	2.73	2.71	2.47	2.61	2.39
Gd	8.18	8.26	8.45	7.76	7.79	7.18
Tb	1.24	1.28	1.30	1.20	1.17	1.13
Dy	7.38	7.56	7.44	7.04	6.78	6.55
Ho	1.41	1.43	1.43	1.34	1.25	1.20
Er	3.89	3.87	3.88	3.76	3.57	3.38
Tm	0.54	0.55	0.56	0.53	0.49	0.49
Yb	3.29	3.39	3.33	3.39	3.11	2.92
Lu	0.48	0.49	0.50	0.49	0.45	0.43
Li	5.70	8.35	6.43	8.83	7.44	18.3
Be	1.98	1.72	1.84	1.81	1.48	1.34
Ga	22.7	22.2	22.6	21.3	20.8	20.7
Sn	2.16	2.07	2.15	1.87	1.83	1.94
Cs	0.29	0.48	0.27	0.71	0.22	0.46
Tl	0.050	0.015	0.050	0.029	0.030	0.041

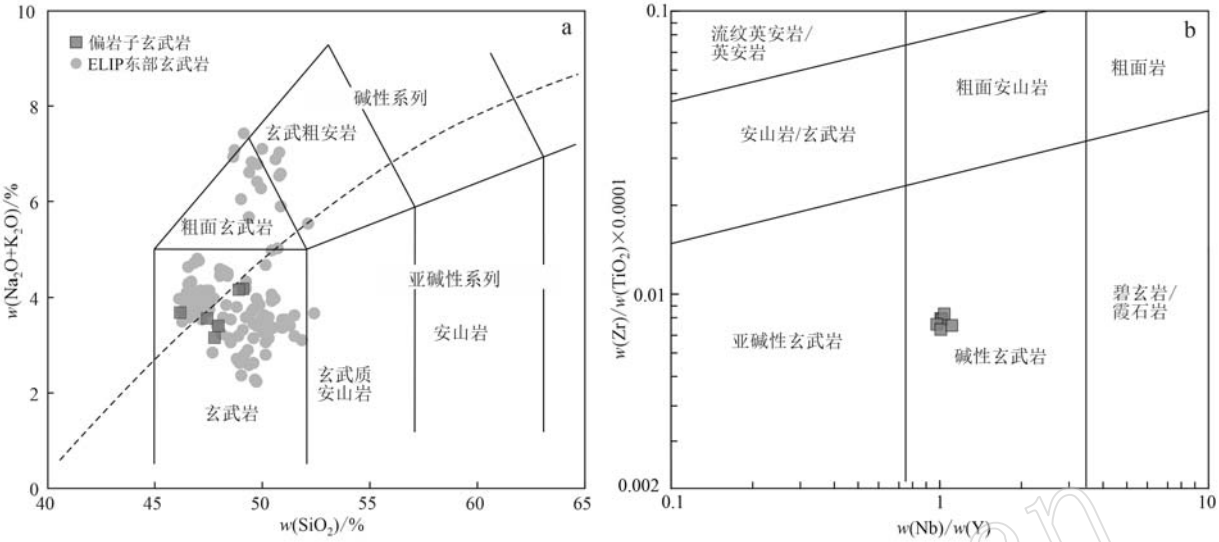

图 5　四川偏岩子晚二叠世玄武岩 TAS 图解[a，碱性/亚碱性界线据 Irvine 和 Baragar（1971），ELIP 东部玄武岩数据引自 Qi 和 Zhou（2008）、Fan 等（2008）、Lai 等(2012)和廖宝丽等(2012)]和 Zr/TiO_2 - Nb/Y 图解[b，Winchester 和 Floyd(1977)]

Fig. 5　TAS diagram(a, alkaline/subalkaline boundary are from Irvine and Baragar, 1971; data of eastern ELIP basalts are from Qi and Zhou, 2008; Fan *et al.*, 2008; Lai *et al.*, 2012 and Liao Baoli *et al.*, 2012) and Zr/TiO_2 - Nb/Y diagram (b, after Winchester and Floyd, 1977) of Late Permian Pianyanzi basalts

偏岩子玄武岩较低的 Ni(46.4×10^{-6}～51.6×10^{-6})和 Cr(33.3×10^{-6}～38.0×10^{-6})含量以及轻微的 Eu 负异常和 Sr 负异常(表 4、图 6a)，表明偏岩子玄武岩经历了大陆溢流玄武岩的典型分离结晶，具有辉长岩分离结晶矿物组合，以辉石和斜长石为主，伴有少量的磁铁矿和橄榄石(Jourdan *et al.*, 2007)。

Nb/U 值是鉴别玄武岩是否受到地壳混染的有效指示剂，大洋玄武岩 Nb/U 值为 47±10，原始地幔 Nb/U 值约为 30，大陆壳 Nb/U 值约为 10，Nb/U 值越低，显示遭受地壳混染程度越大(Hofmann *et al.*, 1986)。偏岩子玄武岩的 Nb/U 值为 24～32，平均 29，与原始地幔值十分接近(表 5)。此外，微量元素蛛网图上也没有 Nb、Ta 等 HFSE 元素的负异常(图 6b)，表明基本没有受到地壳混染。经原始地幔标准化后的 $(Nb/Th)_{PM}$ 值可反映 Nb 异常的程度，而 $(Th/Yb)_{PM}$ 值是地壳混染的灵敏指示剂。在 $(Nb/Th)_{PM}$ -$(Th/Yb)_{PM}$ 图解中，相比于 ELIP 东部其他地区的峨眉山玄武岩(如水城、黑石头等)，偏岩子玄武岩的投点十分靠近峨眉山苦橄岩，也表明偏岩子玄武岩基本未遭受地壳混染的影响(图 7)。总之，偏岩子玄武岩的地壳混染不明显。

4.2　源区特征

由于偏岩子玄武岩经过了一定程度的演化，且成分的变化范围十分有限，因此，难以据此来恢复原始岩浆的情况，也不能估算偏岩子玄武岩地幔源区的地幔潜温(t_p)。然而，玄武岩中斑晶的结晶温度可以约束地幔潜温。如前所述，本文得到的偏岩子玄武岩中单斜辉石斑晶的结晶温度为 1 405～1 439℃，这个温度可能代表了地幔潜温的下限值，因为，原始岩浆自地幔源区上涌至岩浆房的过程中温度会有所下降。与正常的软流圈温度相比较，这个温度要高出约 50～100℃(Mckenzie and Bickle, 1988)。很明显，这暗示了偏岩子地区的岩浆作用存在异常的高温。但与峨眉山苦橄岩所指示的温度异常($\triangle t$)(云南丽江，150～230℃)相比(Zhang *et al.*, 2006)，偏岩子玄武岩的温度异常似乎略低一些，同时也略低于大理苦橄岩(Cai *et al.*, 2020)。根据地幔柱假说，地幔柱轴部(地幔柱尾部通过地幔柱头部中心的地方)的温度最高，其温度异常可达 300±100℃。而地幔柱头部的周边地带，由于是从核幔边界而来的高温物质与较冷的被卷入的下地幔物质混合的产物，其 $\triangle t$ 则要低于地幔柱轴部的温度异常。按照通常的地幔柱浮力通量条件进行计算，其平均 $\triangle t$ 约为 100℃(Griffiths and Campbell, 1990)。由于偏岩子地区处于 ELIP 的外围，远离峨眉山地幔柱的中心(图1b)，相比于峨眉山地幔柱的轴部地区，

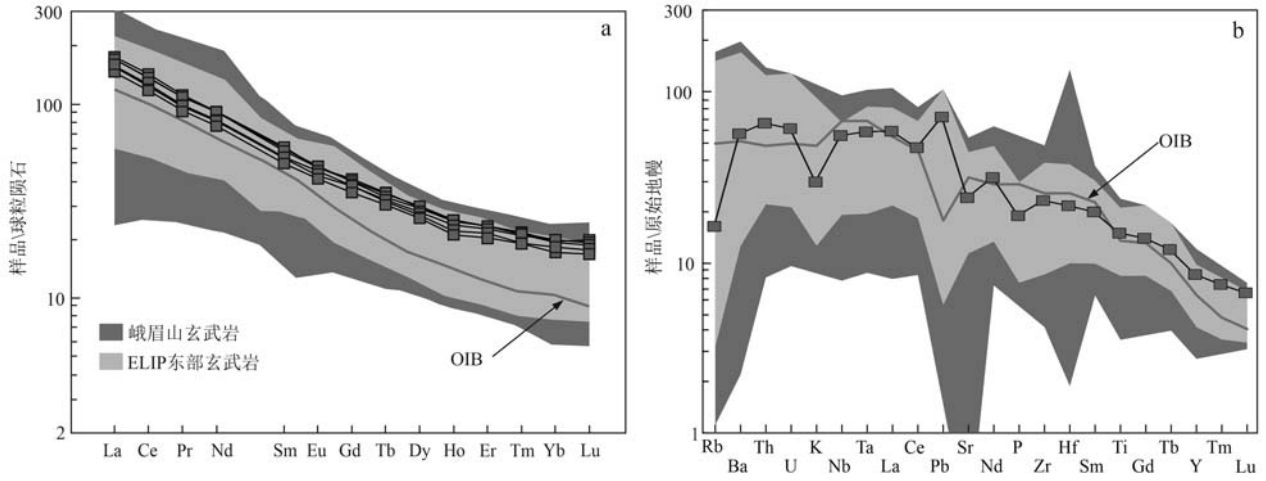

图 6 球粒陨石标准化稀土元素配分曲线(a)和微量元素原始地幔标准化图解(b)

Fig. 6 Chondrite-normalized REE patterns (a) and primitive mantle-normalized trace element spidergrams(b)

标准化数据以及 OIB 根据 Sun 和 McDonough(1989); ELIP 东部玄武岩的数据引自 Zhang 等(2006)、Fan 等(2008)、Qi 和 Zhou(2008)、Lai 等(2012)、廖宝丽等(2012)和 Shellnutt(2014)

Normalizing values and OIB data are from Sun and McDonough, 1989; data of eastern ELIP basalts are from Zhang *et al.*, 2006; Fan *et al.*, 2008; Qi and Zhou, 2008; Lai *et al.*, 2012; Liao *et al.*, 2012 and Shellnutt, 2014

表 5 偏岩子晚二叠世玄武岩与 ELIP 东部玄武岩微量元素比值的对比

Table 5 Comparison of trace element ratios between the Late Permian Pianyanzi basalts and Eastern ELIP basalt

微量元素比值	偏岩子玄武岩	水城(廖宝丽等, 2012)	广西(Lai *et al.*, 2012)	贵州-织金(Lai *et al.*, 2012)	黑石头(Qi and Zhou, 2008)	OIB(Sun and McDonough, 1989)
Th/Nb	0.14	0.15~0.22	0.08~0.23	0.16~0.18	0.14~0.25	0.08
Zr/Nb	6.25~6.62	8.81~10.4	6.00~11.5	8.18~8.77	7.83~10.93	5.83
Nb/La	0.98~1.13	0.64~1.19	0.47~1.05	0.90~0.97	0.77~1.19	1.30
Th/Ta	2.29~2.38	1.78~2.24	1.26~4.81	2.39~2.71	2.04~3.53	1.48
Nb/U	24~32	16~24	25~35	23~26	16~38	47

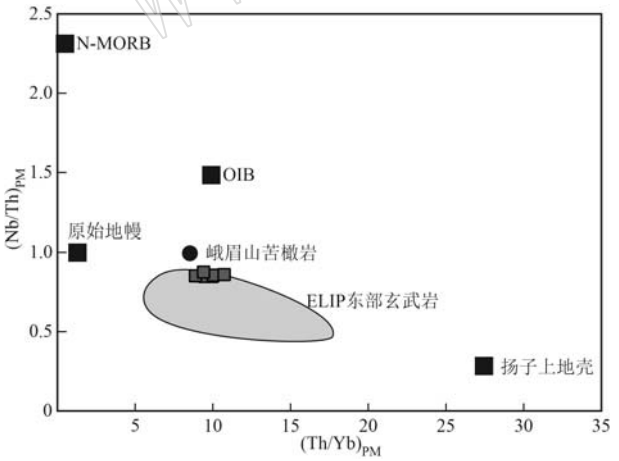

图 7 偏岩子晚二叠世玄武岩的$(Nb/Th)_{PM}$-$(Th/Yb)_{PM}$图解

Fig. 7 $(Nb/Th)_{PM}$-$(Th/Yb)_{PM}$ diagram of Late Permian Pianyanzi basalts

原始地幔(PM)、N-MORB、OIB 引自 Sun 和 McDonough (1989); 峨眉山苦橄岩引自张招崇等(2004)和 Zhang 等 (2006); ELIP 东部玄武岩引自 Qi 和 Zhou (2008)、廖宝丽等 (2012)和 Lai 等(2012); 扬子上地壳引自 Gao 等(1999)和 Ma 等(2000)

PM, N-MORB and OIB (Sun and McDonough, 1989), Emeishan picrite (Zhang Zhaochong *et al.*, 2004; Zhang *et al.*, 2006), eastern ELIP basalts (Qi and Zhou, 2008; Liao Baoli *et al.*, 2012; Lai *et al.*, 2012); the Yangtze upper crust (Gao *et al.*, 1999; Ma *et al.*, 2000)

偏岩子玄武岩的地幔潜温要低一些,这与地幔柱的假说是吻合的。因此,结合偏岩子玄武岩具有与峨眉山玄武岩相似的 OIB 型地球化学特征,认为其较高的源区温度应该指示了地幔柱的存在。

偏岩子玄武岩的 MREE/HREE 分异不强烈,其$(Tb/Yb)_N = 1.61 \sim 1.79$,而近于水平的 HREE[$(Dy/Yb)_N = 1.35 \sim 1.46$]配分模式,也表明 HREE 分异不强,这似乎指示了偏岩子玄武岩源区为石榴子石-尖晶石相过渡区。在 La/Sm - Sm/Yb 投图中,偏岩子玄武岩落在了石榴子石二辉橄榄岩熔融线和尖晶石二辉橄榄岩熔融线之间,略偏石榴子石熔融线(图 8a)。大量的地球化学和地球物理的研究数据表明,熔融深度对熔体的部分熔融程度具有明显的控制作用(Niu and Batiza, 1991; Ellam, 1992; DePaolo and Daley, 2000)。$(Yb/Sm)_{PM}$-$(Tb/Yb)_{PM}$图解可以用来对部分熔融程度以及源区特征进行量化约束(Zhang *et al.*, 2006),图 8b 显示偏岩子玄武岩经历了约 3%~5%的部分熔融,其熔体中来自石榴子石源

区的熔体有40%~60%的贡献。与EILP东部玄武岩相比，偏岩子玄武岩的部分熔融程度相似，但是其源区中石榴子石的比例略小一些，暗示源区较浅一些，可能为石榴子石-尖晶石相过渡区（图8b）。

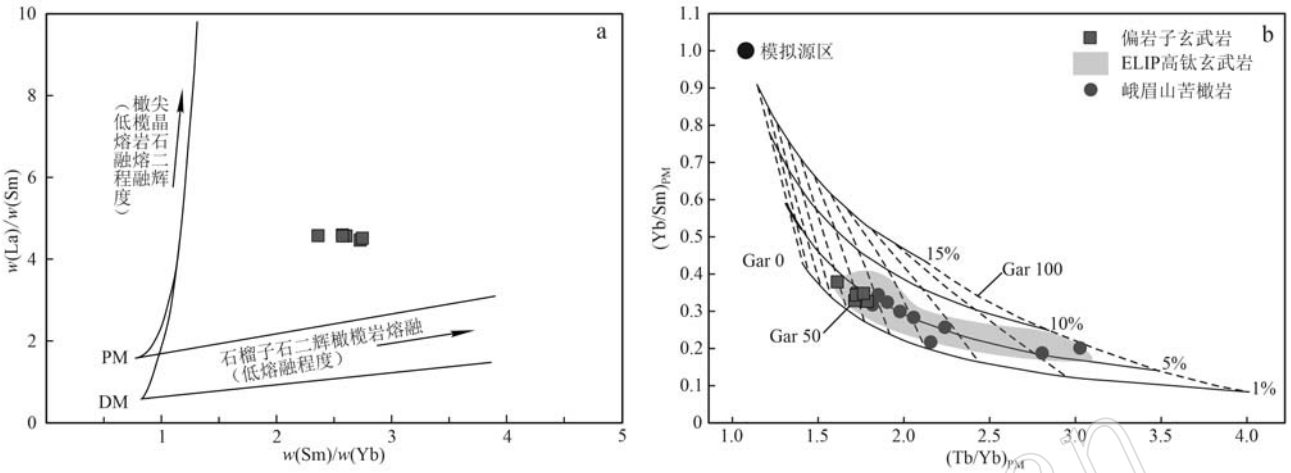

图 8　偏岩子晚二叠世玄武岩的 La/Sm－Sm/Yb 图解[a，据 Lassiter 和 Depaolo（1997）]和$(Yb/Sm)_{PM}$－$(Tb/Yb)_{PM}$图解[b，修改自 Zhang 等(2006)]

Fig. 8　La/Sm－Sm/Yb diagram (a, after Lassiter and Depaolo, 1997) and $(Yb/Sm)_{PM}$－$(Tb/Yb)_{PM}$ diagram (b, modified from Zhang *et al.*, 2006) for Late Permian Pianyanzi basalts

ELIP 高钛玄武岩引自 Xu 等(2001)、Xiao 等(2004a)、Zhang 等（2006）、Wang 等(2007)、Song 等(2008)、Fan 等(2008)、Qi 和 Zhou（2008）、Lai 等(2012)；峨眉山苦橄岩引自张招崇等(2004)和 Zhang 等(2006)

Data sources: Emeishan high-Ti basalts (Xu *et al.*, 2001; Xiao *et al.*, 2004a; Zhang *et al.*, 2006; Wang *et al.*, 2007; Song *et al.*, 2008; Fan *et al.*, 2008; Qi and Zhou, 2008 and Lai *et al.*, 2012); Emeishan picrite (Zhang Zhaochong *et al.*, 2004; Zhang *et al.*, 2006)

经典地幔柱理论认为，由于远离地幔柱中心、地幔柱活动强度较弱、上覆岩石圈较厚等原因，使得地幔柱边缘地区的地幔熔融区间较深（石榴子石稳定区）(Xu *et al.*, 2001)。然而，偏岩子地区晚二叠世火山岩的源区特征似乎与之不符。如前所述，华蓥山深大断裂带对玄武岩质熔岩的喷发有控制作用，峨眉山地幔柱与岩石圈的相互作用可能会在断裂带处形成一个薄弱带。正是这个岩石圈薄弱带使得偏岩子玄武岩的源区较浅。

4.3　成因模型以及对 ELIP 的指示意义

从地层对比和地质产出特征来看，四川偏岩子玄武岩与峨眉山玄武岩是可以对比的，形成时代大致相当（图2、图3）。偏岩子玄武岩为高钛亲碱性的玄武岩，这与 ELIP 东部玄武岩多为碱性玄武岩的特征是一致的(Fan *et al.*, 2008; Qi and Zhou, 2008; 廖宝丽等, 2012; Lai *et al.*, 2012)。从 REE、微量元素的配分模型以及一些微量元素比值来看，偏岩子玄武岩与 ELIP 东部玄武岩以及 OIB 十分相似，并且它们的一些微量元素比值也十分接近（图5、表5）。总之，无论是岩相学特征、主微量元素，偏岩子玄武岩均与峨眉山玄武岩，尤其是 ELIP 东部的玄武岩表现出相似性（图6~图8、表5），因此，偏岩子玄武岩与峨眉山玄武岩是同源的产物，是 ELIP 的组成部分。

基于以上对偏岩子玄武岩源区特征以及与峨眉山玄武岩成因关系的分析，可以提出如下的成因模型：晚二叠世（~260 Ma），在扬子克拉通西缘，发生了大陆溢流玄武岩质岩浆作用。偏岩子地区位于 ELIP 的周边地带，远离地幔柱轴部，地幔柱的高温异常相对弱一些，但是还是导致了岩浆作用的发生。地幔柱与岩石圈地幔相互作用下，在石榴子石-尖晶石过渡区，经较低程度的部分熔融，产生了亲碱性高钛的玄武岩质岩浆。岩浆沿着华蓥山深大断裂上涌，喷出地表形成了偏岩子玄武岩。

由于漫长地质历史中的风化剥蚀作用、上覆地层的掩埋以及深部岩体（pluming system）难以探测等原因，目前对 LIP（尤其是古老的 LIP）分布面积的认识很可能只是冰山一角(Ernst, 2014)。近年来，由于一些新组成部分的不断发现，使得 LIPs 的面积不断被刷新，如西伯利亚 LIP(Reichow *et al.*, 2002; Ivanov, 2007)、Ontong Java 大洋 LIP(Ingle and Coffin, 2004; Taylor, 2006)、Comei-Bundury LIP(Zhu *et*

al., 2009)等。

ELIP东部的玄武岩主要分布于扬子克拉通之内的广大地区,传统认为该岩区的空间展布分别受西侧小江断裂,东北侧宝兴–宜宾断裂和东南侧弥勒–斯宗断裂的控制(宋谢炎等, 2002; 图1)。尽管在宝兴–宜宾断裂以东的地区,区域调查以及石油钻孔显示有晚二叠世玄武岩存在,但一直未得到相关研究的证实(童崇光, 1992; Ma *et al.*, 2008)。本文通过矿物学和地球化学特征的研究表明,偏岩子晚二叠世玄武岩与峨眉山玄武岩是同源产物,属于ELIP的组成部分。

此外,Zhu等(2010, 2016)对四川盆地的热流史的研究表明,四川盆地在259 Ma左右,盆地的古热流值和古地热梯度达到最高(偏岩子附近的Nj井的古热流值为67.8 W/m^2),高热流值的时空分布与峨眉山玄武岩的火山作用具有很好的相关性,表明与峨眉山地幔柱的活动有关。刘兴兵等(2013)、田和明等(2014)分别对重庆南川晚二叠世凝灰岩以及上二叠统硫铁矿进行了研究,结果表明无论是凝灰岩还是硫铁矿均可能与ELIP的基性岩浆作用有关。

偏岩子玄武岩的发现以及这些证据表明,ELIP岩浆作用的影响波及了四川盆地的广大地区(Li *et al.*, 2017)。

5 结论

四川偏岩子晚二叠世玄武岩在地层上可与峨眉山玄武岩对比,是同期产物。主微量地球化学特征表明,偏岩子玄武岩属于高钛亲碱性系列,并具有OIB型的REE和微量元素配分模式,与ELIP东部的玄武岩相似。偏岩子玄武岩基本未受到地壳混染的影响。单斜辉石温度计、微量元素比值判别图表明,偏岩子玄武岩是峨眉山地幔柱在石榴子石–尖晶石区经较低程度的部分熔融产生的,是ELIP的组成部分。偏岩子玄武岩的发现再次表明ELIP岩浆作用的影响波及了四川盆地的广大地区。

References

Ali J R, Lo C H, Thompson G M, *et al*. 2004. Emeishan basalt Ar-Ar overprint ages define several tectonic events that affected the western Yangtze platform in the Mesozoic Cenozoic[J]. J. Asian Earth Sci., 23: 163~178.

Bryan S E and Ernst R E. 2008. Revised definition of Large Igneous Provinces (LIPs)[J]. Earth-Science Reviews. 86 (1~4): 175~202.

Cai W C, Zhang Z C, Zhu J, *et al*. 2020. Genesis of high-Ni olivine phenocrysts of the Dali picrites in the Central Emeishan large igneous province[J]. Geological Magazine, 158: 985~994.

Campbell I H and Griffiths R W. 1990. Implications of mantle plume structure for the evolution of flood basalts[J]. Earth and Planetary Science Letters, 99 (1~2): 79~93.

Campbell I H. 1998. The mantle's chemical structure: Insights from the melting products of mantle plumes[A]. The Earth's Mantle: Composition, Structure and Evolution[C]. Jackson I N S. New York: Cambridge University, 259~310.

Campbell I H. 2001. Identification of ancient mantle plumes[A]. Ernst R E and Buchan K L. Mantle Plumes: Their Identification Through Time[C]. Boulder: Geological Society of America, 5~21.

Chen Hui, Deng Jianghong, Liu Shugen, *et al*. 2019. Basalt characteristics of Well Ys-1 in western Sichuan and contrast with Emeishan basalts[J]. Journal of Chengdu University of Technology (Science & Technology Edition), 46: 299 ~ 315 (in Chinese with English abstract).

Chen Y, Xu Y G, Xu T, *et al*. 2015. Magmatic underplating and crustal growth in the Emeishan Large Igneous Province, SW China, revealed by a passive seismic experiment[J]. Earth and Planetary Science Letters, 432: 103~114.

Chung S L, Jahn B M, Wu G Y, *et al*. 1998. The Emeishan flood basalt in SW China: A mantle plume initiation model and its connection with continental breakup and mass extinction at the Permian-Triassic boundary[J]. AGU Geodynamics Series, 27: 47~58.

Chung S L and Jahn B M. 1995. Plume-lithosphere interaction in generation of the Emeishan flood basalts at the Permian-Trassic boundary [J]. Geology, 23 (10): 889~892.

Coffin M F and Eldholm O. 1994. Large igneous provinces: Crustal structure, dimensions and external consequences[J]. Reviews of Geophysics, 32: 1~36.

Coffin M F and Eldholm O. 2001. Large igneous provinces: progenitors of some ophiolites? [A]. Ernst R E and Buchan K L. Mantle Plumes: Their Identification Through Time[C]. Boulder: Geological Society of America, 59~70.

Cordery M J, Davies G F and Campbell I H. 1997. Genesis of flood basalts from eclogite-bearing mantle plumes[J]. Journal of Geophysics Research, 102: 20 179~20 197.

Courtillot V, Davaille A, Besse J, *et al*. 2003. Three distinct types of

hotspots in the Earth's mantle[J]. Earth and Planetary Science Letters, 205: 295~308.

Courtillot V, Jaupart C, Manighetti I, *et al*. 1999. On causal links between flood basalts and continental breakup[J]. Earth and Planetary Science Letters, 166: 177~195.

Davies G F. 2000. Dynamic Earth, Plates Plumes and Mantle Convection [J]. Physics Today, 53 (11): 53~54.

DePaolo D J and Daley E E. 2000. Neodymium isotopes in basalts of the southwest basin and range and lithospheric thinning during continental extension[J]. Chem. Geol., 169: 157~185.

Ellam R M. 1992. Lithospheric thickness as a control on basalt geochemistry[J]. Geology, 20: 153~156.

Ernst R E and Buchan K L. 2001a. The use of mafic dike swarms in identifying and locating mantle plumes[A]. Ernst R E and Buchan K L. Mantle Plumes: Their Identification Through Time [C]. Boulder: Geological Society of America, 247~265.

Ernst R E and Buchan K L. 2001b. Large mafic magmatic events through time and links to mantle-plume heads[A]. Ernst R E and Buchan K L. Mantle Plumes: Their Identification Through Time[C]. Boulder: Geological Society of America, 483~575.

Ernst R E and Buchan K L. 2002. Maximum size and distribution in time and space of mantle plumes: Evidence from large igneous provinces [J]. Journal of Geodynamics, 34 (2): 309~342.

Ernst R E and Buchan K L. 2003. Recognizing mantle plumes in the geological record[J]. Earth and Planetary Science Letters, 31: 469~523.

Ernst R E, Buchan K L and Campbell I H. 2005. Frontiers in Large Igneous Province research[J]. Lithos, 79: 271~297.

Ernst R E. 2014. Large Igneous Provinces[M]. Cambridge University Press, 281: 41~42.

Fan W M, Zhang C H, Wang Y J, *et al*. 2008. Geochronology and geochemistry of Permian basalts in western Guangxi Province, Southwest China: Evidence for plume-lithosphere interaction[J]. Lithos, 102(1~2): 218~236.

Farnetani C G. 1996. Excess temperature of mantle plumes: The role of chemical stratification across D"[J]. Geophys Research Letters, 24: 1 583~1 586.

Farnetani C G and Richards M A. 1994. Numerical investigations of the mantle plume initiation model for flood basalt events[J]. Journal of Geophysics Research, 99: 13 813~13 833.

Gao S, Ling W L, Qiu Y M, *et al*. 1999. Contrasting geochemical and Sm-Nd isotopic compositions of Archean metasediments from the Kongling high-grade terrain of the Yangtze craton: Evidence for cratonic evolution and redistribution of REE during crustal anatexis [J]. Geochimica et Cosmochimica Acta, 63: 2 071~2 088.

Griffiths R W and Campbell I H. 1990. Stirring and structure in mantle plumes[J]. Earth and Planetary Science Letters, 99: 66~78.

Griffiths R W and Campbell I H. 1991. On the dynamics of long-lived plume conduits in the convecting mantle[J]. Earth and Planetary Science Letters, 103(1~4): 214~227.

Griffiths R W, Gurnis M and Eitelberg G. 1989. Holographic measurements of surface-topography in laboratory models of mantle hotspots [J]. Geophysical Journal of the Royal Astronomical Society, 96(3): 477~495.

Hames W E, McHone J G, Renne P R, *et al*. 2003. The Central Atlantic Magmatic Province: Insights from fragments of Pangea[J]. American Geophysical Union, Geophysical Monograph, 136: 267.

Hanski E, Kamenetsky V S, Luo Z Y, *et al*. 2010. Primitive magmas in the Emeishan Large Igneous Province, southwestern China and northern Vietnam[J]. Lithos, 119: 75~90.

Hanski E, Walker R J, Huhma H, *et al*. 2004. Origin of Permian-Triassic komatiites, northwestern Vietnam[J]. Contributions to Mineralogy and Petrology, 147: 453~469.

He B, Xu Y G, Chung S L, *et al*. 2003. Sedimentary evidence for a rapid, kilometer-scale crustal doming prior to the eruption of the Emeishan flood basalts[J]. Earth and Planetary Science Letters, 213(3~4): 391~405.

He B, Xu Y G, Huang X L, *et al*. 2007. Age and duration of the Emeishan flood volcanism, SW China: Geochemistry and SHRIMP zircon U-Pb dating of silicic ignimbrites, post-volcanic Xuanwei Formation and clay tuff at the Chaotian section[J]. Earth and Planetary Science Letters, 255 (3~4): 306~323.

Hill R I. 1991. Starting plumes and continental break-up[J]. Earth and Planetary Science Letters, 104: 398~416.

Hofmann A W, Jochum K P, Seufert M, *et al*. 1986. Nb and Pb in oceanic basalts: New constraints on mantle evolution [J]. Earth and Planetary Science Letters, 79: 33~45.

Ingle S and Coffin M F. 2004. Impact origin for the greater ontong java plateau? [J]. Earth and Planetary Science Letters, 218: 123~134.

Irvine T N and Baragar W R A. 1971. A guide to the chemical classification of the common volcanic rocks[J]. Canadian Journal of Earth Sciences, 8(5): 523~548.

Ivanov A V. 2007. Evaluation of different models for the origin of the Siberian Traps[A]. Foulger G R and Jurdy D M. The Origins of Melting Anomalies: Plates, Plumes, and Planetary Processes[C]. Geological Society of America, 669~691.

Jourdan F, Bertrand H, Schärer U, *et al*. 2007. Major and trace element and Sr, Nd, Hf, and Pb isotope compositions of the Karoo Large Igneous Province, Botswana-Zimbabwe: Lithosphere vs Mantle Plume Contribution[J]. Journal of Petrology, 48: 1 043~1 077.

Kincaid C, Sparks D W and Detrick R. 1996. The relative importance of plate-driven and buoyaney-driven flow at mid-ocean ridges[J]. Journal of Geophysical Research, 101: 16 177~16 193.

Lai S C, Qin J F, Li Y F, *et al*. 2012. Permian high Ti/Y basalts from the eastern part of the Emeishan Large Igneous Province, southwestern China: Petrogenesis and tectonic implications[J]. J. Asian Earth Sci., 47: 216~230.

Lassiter J C and Depaolo D J. 1997. Plume/lithosphere interaction in the generation of continental and oceanic flood basalts: Chemical and isotope constraints[A]. Mahoney J. Large Igneous Provinces: Continental, Oceanic and Planetary Flood Volcanism[M]. American Geophysical Union Geophysical Monography, 100: 335~355.

Li H B, Zhang Z C, Ernst R, *et al*. 2015. Giant radiating mafic dyke swarm of the Emeishan Large Igneous Province: Identifying the mantle plume centre[J]. Terra Nova, 27: 247~257.

Li Hongbo, Zhang Zhaochong and Li Yongsheng. 2015. Geochronology and geochemistry of the Late Permian intermediary-mafic intrusions in Fumin, Yunnan Province: Implications for the magmatism of Emeishan large igneous province[J]. Acta Geologica Sinica, 89: 18~36 (in Chinese with English abstract).

Li Hongbo, Zhang Zhaochong and Lü Linsu. 2010. Geometry of the mafic dyke swarms in Emeishan large igneous province: Implications formantle plume[J]. Acta Petrologica Sinica, 26: 3 143~3 152(in Chinese with English abstract).

Li Hongbo, Zhang Zhaochong, Lü Linsu, *et al*. 2011. Isopach maps of the Qixia and Maokou Formations: Implication for mantle plume model of the Emeishan large igneous province[J]. Acta Petrologica Sinica, 27: 2 963~2 974 (in Chinese with English abstract).

Li Hongbo, Zhang Zhaochong, Lü Linsu, *et al*. 2012. Geochronology, geochemistry and geologic significances of the Permian mafic dykes in Mianning, Sichuan Province[J]. Geological Review, 58: 952~964 (in Chinese with English abstract).

Li H B, Zhang Z C, Santosh M, *et al*. 2016. Late Permian basalts in the northwestern margin of the Emeishan Large Igneous Province: Implications for the origin of the Songpan-Ganzi terrane[J]. Lithos, 256~257: 75~87.

Li H B, Zhang Z C, Santosh M, *et al*. 2017. Late Permian basalts in the Yanghe area, eastern Sichuan Province, SW China: Implications for the geodynamics of the Emeishan flood basalt province and Permian global mass extinction[J]. Journal of Asian Earth Sciences, 134: 293~308.

Li Hongkui. 2020. Study on the Geological Structure and Superimposed Characteristics of Sichuan Basin[D]. Sichuan: Chengdu University of Technolog(in Chinese).

Liao Baoli, Zhang Zhaochong, Kou Caihua, *et al*. 2012. Geochemistry of the Shuicheng Permian sodium trachybasalts in Guizhou Province and constraints on the mantle sources[J]. Acta Petrologica Sinica, 28(4): 1 238~1 250(in Chinese with English abstract).

Liu Deliang, Song Yan, Xue Aimin, *et al*. 2000. Comprehensive Study on Structure and Natural Gas Accumulation Zone in Sichuan Basin [M]. Beijing: Petroleum Industry Press(in Chinese).

Liu Ran, Luo Bing, Li Ya, *et al*. 2021. Relationship between Permian volcanic rocks distribution and karst paleogeomorphology of Maokou Formation and its significance for petroleum exploration in western Sichuan Basin, SW China[J]. Petroleum Exploration and Development, 48(3): 575~585(in Chinese with English abstract).

Liu Xingbing, Cheng Jun, Tang Benfeng, *et al*. 2013. Upper Permian sedimentary environment and metallogenic model of pyrite in Chongqing[J]. Geological Science and Technology Information, 32: 148~154(in Chinese with English abstract).

Lü Jinsong, Xiao Yuanfu, Deng Jianghong, *et al*. 2013. A comparative study of Emeishan basalt and Gangdagai Formation basalt in northwest Yunnan Province[J]. Acta Petrologica et Mineralogica, 32: 73~89 (in Chinese with English abstract).

Ma C Q, Ehlers C, Xu C H, *et al*. 2000. The roots of the Dabieshan ultrahigh-pressure metamorphic terrane: Constraints from geochemistry and Nd-Sr isotope systematics[J]. Precambrian Research, 102 : 279~301.

Ma X H, Li G H, Ying D L, *et al*. 2019. Distribution and gas-bearing properties of Permian igneous rocks in Sichuan Basin, SW China[J]. Petrol. Explor. Dev., 46: 1~10.

Ma Y S, Zhang S C, Guo T L, *et al*. 2008. Petroleum geology of the Puguang sour gas field in the Sichuan Basin, SW China[J]. Marine and Petroleum Geology, 25: 357~370.

Mckenzie D and Bickle M J. 1988. The volume and composition of melt generated by extension of the lithosphere[J]. Journal of Petrology, 29: 625~679.

Morimoto N, Fabries J, Ferguson, A K, *et al*. 1988. Nomenclature of pyroxene[J]. American Mineralogy, 73: 1123~1133.

Niu Y L and Batiza R. 1991. An empirical method for calculating melt compositions produced beneath mid-ocean ridges: application for axis and off-axis (seamounts) melting[J]. J. Geophys. Res., 96:

21 753~21 777.

Olsen P E. 1999. Giant lava flows, mass extinctions, and mantle plumes [J]. Science, 284: 604~605.

Polyakov G V, Balykin P A, Tran T H, *et al*. 1998. Evolution of the Mesozoic-Cenozoic magmatism in the Song Da rift and its contouring structures (northwestern Vietnam) [J]. Russian Geology and Geophysics, 39: 695~706 (in Russian).

Putirka K D, Mikaelian H, Ryerson F, *et al*. 2003. New clinopyroxene liquid thermobarometer for mafic, evolved, and volatile-bearing lava composition, with applications to lavas from Tibet and Snake River Plain, Idaho[J]. American Mineralogy, 88: 1 542~1 554.

Qi L and Zhou M F. 2008. Platinum-group elemental and Sr-Nd-Os isotopic geochemistry of Permian Emeishan flood basalts in Guizhou Province, SW China[J]. Chem. Geol., 248: 83~103.

Qin Jianxiong, Chen Hongde and Tian Jingchun. 1999. Permian sequence paleogeographic characteristics and evolution in southwestern China[J]. Regional Geology of China, 18: 289~297 (in Chinese with English abstract).

Reichow M K, Saunders A D, White R V, *et al*. 2002. $^{40}Ar/^{39}Ar$ dates from the West Siberian Basin: Siberian flood basalt province doubled [J]. Science, 296 (5574): 1 846~1 849.

Shellnutt J G, Denyszyn S W and Mundil C R. 2012. Precise age determination of mafic and felsic intrusive rocks from the Permian Emeishan large igneous province (SW China) [J]. Gondwana Research, 22 (1): 118~126.

Shellnutt J G, Zhou M F, Yan D P, *et al*. 2008. Longevity of the Permian Emeishan mantle plume (SW China): 1 Ma, 8 Ma or 18 Ma? [J]. Geological Magzine, 145: 373~388.

Shellnutt J G. 2014. The Emeishan large igneous province: A synthesis [J]. Geoscience Frontiers, 5: 369~394.

Sheth H C. 2007. 'Large Igneous Provinces (LIPs)': Definition, recommended terminology, and a hierarchical classification[J]. Earth-Science Reviews, 85: 117~124.

Smith J V and Brown W L. 1974. Feldspar Minerals[J]. Germany: Springer-Verlag, 1~690.

Song X Y, Qi H W, Robinson P T, *et al*. 2008. Melting of the subcontinental lithospheric mantle by the Emeishan mantle plume: Evidence from the basal alkaline basalts in Dongchuan, Yunnan, Southwestern China[J]. Lithos 100: 93~111.

Song X Y, Zhou M F, Cao Z M, *et al*. 2004. Late Permian rifting of the South China Craton caused by the Emeishan mantle plume? [J]. Journal of Geological Society, 161(5): 773~781.

Song Xieyan, Hou Zhengqian, Wang Yunliang, *et al*. 2002. The mantle plume features of Emeishan basalts[J]. J. Mineral. Petrol., 22: 27~32(in Chinese with English abstract).

Sun S S and McDonough W F. 1989. Chemical and isotopic systematics of oceanic basalt: Implications for mantle composition and processes [A]. Sanders A D and Norry M J. Magmatism in the Ocean Basins 42 [C]. Geological Society Special Publication, London, 313~345.

Taylor B. 2006. The single largest oceanic plateau: Ontong Java-Manihiki-Hikurangi[J]. Earth and Planetary Science Letters, 241: 372~380.

Tian Heming, Dai Shifeng, Li Dahua, *et al*. 2014. Geochemical features of the late Permian tuff in Nanchuan district, Chongqing, southwestern China[J]. Geol. Rev., 60: 169~177(in Chinese with English abstract).

Tong Chongguan. 1992. Tectonic Evolution and Hydrocarbon Accumulation in Sichuan Basin[M]. Beijing: Geological Publishing House(in Chinese).

Wang C Y, Zhou M F and Qi L. 2007. Permian flood basalts and mafic intrusions in the Jinping(SW China)-Song Da (northern Vietnam) district: Manlte source, crustal contamination and sufide segregation [J]. Chemical Geology, 243: 317~343.

Wen L, Li Y, Yi H Y, *et al*. 2019. Lithofacies and reservoir characteristics of permian volcanic rocks in the sichuan basin[J]. Natural Gas Industry B, 6: 452~462.

Winchester J A and Floyd P A. 1977. Geochemical discrimination of different magma series and their differentiation products using immobile elements[J]. Chemical Geology, 20: 325~343.

Xiang F, Yu X, Huang H, *et al*. 2021. Mineralogical characterization and diagenetic history of Permian marine tuffaceous deposits in Guangyuan area, northern Sichuan basin, China[J]. Marine and Petroleum Geology, 123: 104 744.

Xiao L, Xu Y G, Mei H J, *et al*. 2004a. Distinct mantle sources of low-Ti and high-Ti basalts from the western Emeishan large igneous provinces, SW China: Implications of plumelithosphere interaction[J]. Earth and Planetary Science Letters, 228 (3~4): 525~546.

Xiao L, Xu Y G, Xu J F, *et al*. 2004b. Chemostratigraphy of flood basalts in the Garze-Litang region and Zongza block: Implications for western extension of the Emeishan large igneous province, SW China [J]. Acta Geologica Sinica, 78(1): 61~67.

Xiao Long, Xu Yigang, Mei Houjun, *et al*. 2003. Late Permian flood basalts at Jinping area and its relation to Emei mantle plume: Geochemical evidences[J]. Acta Petrol. Sin., 19: 38~48(in Chinese with English abstract).

Xu Y G, Chung S L, Jahn B M, *et al*. 2001. Petrologic and geochemical

constraints on the petrogenesis of Permian-Triassic Emeishan flood basalts in southwestern China[J]. Lithos, 58 (3~4): 145~168.

Xu Y G, He B, Chung S L, *et al*. 2004. Geologic, geochemical, and geophysical consequences of plume involvement in the Emeishan flood-basalt province[J]. Geology, 32: 917~920.

Xu Y G, Luo Z Y, Huang X L, *et al*. 2008. Zircon U-Pb and Hf isotope constraints on crustal melting associated with the Emeishan mantle plume[J]. Geochimica et Cosmochimica Acta, 72: 3 084~3 104.

Yin Jifeng, Gu Zhidong and Li Qiufen. 2013. Characteristics of deep-rooted faults and their geological signifcances in Dachuanzhong area, Sichuan Basin[J]. Oil Gas Geol., 34: 376~382(in Chinese with English abstract).

Zhang Yunxiang, Luo Yaonan and Yang Chongxi. 1988. Panxi Rift and Its Geodynamics[M]. Beijing: Geological Publishing House(in Chinese).

Zhang Zhaochong. 2009. A discussion on some important problems concerning the Emeishan large igneous province[J]. Geology in China, 36: 634~646(in Chinese with English abstract).

Zhang Z C, Mahoney J J, Mao J W, *et al*. 2006. Geochemistry of picritic and associated basalt flows of the western Emeishan flood basalt province, China[J]. Journal of Petrology, 47 (10): 1 997~2 019.

Zhang Zhaochong, Wang Fusheng, Hao Yanli, *et al*. 2004. Geochemistry of the picrites and associated basalts from the Emeishan large igneous basalt province and constraints on their source region[J]. Acta Geologica Sinica, 78: 171~180(in Chinese with English abstract).

Zhang Z C, Zhi X C, Chen L L, *et al*. 2008. Re-Os isotopic compositions of picrites from the Emeishan flood basalt province, China[J]. Earth and Planetary Science Letters, 276(1~2): 30~39.

Zhong H, Yao Y, Prevec S A, *et al*. 2004. Trace-element and Sr-Nd isotopic geochemistry of the PGE-bearing Xinjie layered intrusion in SW China[J]. Chem. Geol., 203 (3~4): 237~252.

Zhong Y T, He B, Mundil R, *et al*. 2014. CA-TIMS zircon U-Pb dating of felsic ignimbrite from the Binchuan section: implications for the termination age of Emeishan large igneous province[J]. Lithos, 204: 14~19.

Zhou M F, Arndt N T, Malpas J, *et al*. 2008. Two magma series and associated ore deposit types in the Permian Emeishan large igneous province, SW China[J]. Lithos, 103(3~4): 352~368.

Zhou M F, Malpas J, Song X Y, *et al*. 2002. A temporal link between the Emeishan large igneous province[J]. Earth Planet. Sci. Lett., 196: 113~122.

Zhou M F, Robinson P T, Lesher C M, *et al*. 2005. Geochemistry, petrogenesis and metallogenesis of the Panzhihua gabbroic layered intrusion and associated Fe-Ti-V oxide deposits, Sichuan Province, SW China[J]. Journal of Petrology, 46: 2 253~2 280.

Zhou M F, Zhao J H, Qi L, *et al*. 2006. Zircon U-Pb geochronology and elemental and Sr-Nd isotope geochemistry of Permian mafic rocks in the Funing area, SW China[J]. Contributions to Mineralogy and Petrology, 151(1): 1~19.

Zhu C Q, Hu S B, Qiu N S, *et al*. 2016. The thermal history of the Sichuan Basin, SW China: Evidence from the deep boreholes[J]. Science China Earth Sciences, 59: 70~82.

Zhu C Q, Xu M, Yuan Y S, *et al*. 2010. Palaeogeothermal response and record of the effusing of Emeishan basalts in the Sichuan basin[J]. Chin. Sci. B, 55: 949~956.

Zhu D C, Chung S L, Mo X X, *et al*. 2009. The 132 Ma Comei-Bunbury large igneous province: Remnants identified in present-day SE Tibet and SW Australia[J]. Geology, 37: 583~586.

Zhu J, Zhang Z C, Santosh M, *et al*. 2021a. Recycled carbon degassed from the Emeishan plume as the potential driver for the major end-Guadalupian carbon cycle perturbations[J]. Geoscience Frontiers, 12: 101~140.

Zhu J, Zhang Z C, Santosh M, *et al*. 2021b. Submarine basaltic eruptions across the Guadalupian-Lopingian transition in the Emeishan large igneous province: Implication for end-Guadalupian extinction of marine biota[J]. Gondwana Research, 92: 228~238.

Zhu Jiang, Zhang Zhaochong, Hou Tong, *et al*. 2011. LA-ICP-MS zircon U-Pb geochronology of the tuffs on the uppermost of the Emeishan basalt succession in Panxian County, Guizhou Province: Constraints on genetic link between Emeishan large igneous province and the mass extinction[J]. Acta Petrologica Sinica, 27: 2 743~2 751 (in Chinese with English abstract).

Zi J W, Fan W M, Wang Y J, *et al*. 2010. U-Pb geochronology and geochemistry of the Dashibao basalts in the Songpan-Ganzi terrane, SW China, with implications for the age of Emeishan volcanism[J]. American Journal of Science, 310: 1 054~1 080.

附中文参考文献

陈 辉, 邓江红, 刘树根, 等. 2019. 川西YS-1井玄武岩特征及与峨眉山玄武岩对比[J]. 成都理工大学学报(自然科学版), 46(3): 299~315.

李宏博, 张招崇, 李永生. 2015. 云南富民晚二叠世中-基性岩年代学、地球化学特征: 对峨眉山大火成岩省岩浆作用过程的指示意义[J]. 地质学报, 89(1): 18~36.

李宏博，张招崇，吕林素. 2010. 峨眉山大火成岩省基性岩墙群几何学研究及对地幔柱中心的指示意义[J]. 岩石学报，26(10)：3 143~3 152.

李宏博，张招崇，吕林素，等. 2011. 栖霞组和茅口组等厚图：对峨眉山地幔柱成因模式的指示意义[J]. 岩石学报，27(10)：2 963~2 974.

李宏博，张招崇，吕林素，等. 2012. 四川冕宁基性岩墙的年代学、地球化学特征及其地质意义[J]. 地质论评，58(5)：952~964.

李洪奎. 2020. 四川盆地地质结构及叠合特征研究(博士论文)[D]. 四川：成都理工大学.

廖宝丽，张招崇，寇彩化，等. 2012. 贵州水城二叠纪钠质粗面玄武岩的地球化学特征及其源区[J]. 岩石学报，28(4)：1 238~1 250.

刘德良，宋　岩，薛爱民，等. 2000. 四川盆地构造与天然气聚集区带综合研究[M]. 北京：石油工业出版社，1~6.

刘　冉，罗　冰，李　亚，等. 2021. 川西地区二叠系火山岩展布与茅口组岩溶古地貌关系及其油气勘探意义[J]. 石油勘探与开发，48(3)：575~585.

刘兴兵，程　军，唐本锋，等. 2013. 重庆市上二叠统硫铁矿沉积环境及成矿模式[J]. 地质科技情报，32(1)：148~154.

吕劲松，肖渊甫，邓江红，等. 2013. 滇西北峨眉山玄武岩与冈达概组下段玄武岩对比研究[J]. 岩石矿物学杂志，32(1)：73~89.

宋谢炎，侯增谦，汪云亮，等. 2002. 峨眉山玄武岩的地幔热柱成因[J]. 矿物岩石，22(4)：27~32.

覃建雄，陈洪德，田景春. 1999. 西南地区二叠纪层序古地理特征及演化[J]. 中国区域地质，18(3)：289~297.

田和明，代世峰，李大华，等. 2014. 重庆南川晚二叠世凝灰岩的元素地球化学特征[J]. 地质论评，(1)：169~177.

童崇光. 1992. 四川盆地构造演化与油气聚集[M]. 北京：地质出版社.

肖　龙，徐义刚，梅厚钧，等. 2003. 云南宾川地区峨眉山玄武岩地球化学特征：岩石类型及随时间演化规律[J]. 地质科学，38(4)：478~494.

殷积峰，谷志东，李秋芬. 2013. 四川盆地大川中地区深层断裂发育特征及其地质意义[J]. 石油与天然气地质，34 (3)：376~382.

张云湘，骆耀南，杨崇喜，等. 1988. 攀西裂谷[M]. 北京：地质出版社.

张招崇. 2009. 关于峨眉山大火成岩省一些重要问题的讨论[J]. 中国地质，36(3)：634~646.

张招崇，王福生，郝艳丽. 2004. 峨眉山大火成岩省中苦橄岩与其共生岩石的地球化学特征及其对源区的约束[J]. 地质学报，78(2)：171~180.

宋　江，张招崇，侯　通，等，2011. 贵州盘县峨眉山玄武岩系顶部凝灰岩 LA-ICP-MS 锆石 U-Pb 年龄：对峨眉山大火成岩省与生物大规模灭绝关系的约束[J]. 岩石学报，27(9)：2 743~2 751.